

Influence of pulse electrodeposition parameters on microhardness, grain size and surface morphology of Ni–Co/SiO₂ nanocomposite coating

SIAVASH IMANIAN GHAZANLOU^{1,*}, ALI SHOKUHFAR¹, SHIVA NAVAZANI¹
and REZVAN YAVARI²

¹Advanced Materials and Nanotechnology Research Laboratory, Faculty of Materials
Science and Engineering, K. N. Toosi University of Technology, Tehran 1969764499, Iran

²Faculty of Materials and Metallurgy Engineering, Semnan 35131-19111, Iran

MS received 3 November 2015; accepted 17 March 2016

Abstract. Ni–Co/SiO₂ nanocomposite coatings and Ni–Co alloy coatings were prepared on steel substrate using direct and pulse electrodeposition methods. X-ray diffraction (XRD), field emission scanning electron microscope (FESEM), X-ray map and energy dispersive X-ray spectroscopy (EDX) were employed to investigate the phase structure, surface morphology, and elemental analysis of coatings, respectively. In high discharge rates, the surface morphology was rough, disordered and gross globular; on the contrary, in the low rates, it was smoother, more ordered and fine globular. Also, effect of electrodeposition parameters such as average current density, pulse frequency and duty cycle on the microhardness and grain size of nanocomposite coatings that produced through the pulse current electrodeposition method have been investigated. By amplifying both duty cycles up to 50% and average current density from 2 to 6 A dm⁻², microhardness increased, while the grain size decreased. But when duty cycle mounted on more than 50% and the average current density went up to 8 A dm⁻², microhardness lessened, while the grain size rose. The optimum value for pulse frequency was about 25 Hz. Results showed that microhardness of nanocomposite coatings which were produced by pulse current method was higher than that of produced by direct current method.

Keywords. Nanocomposite coating; electrodeposition; average current density; pulse frequency; duty cycle.

1. Introduction

One of the best methods to produce nanostructure coatings is electrodeposition method, in which discharge is performed on the cathode. Nucleation on the cathode is affected by different agents such as crystal structure of the substrate, surface free energy, adhesion energy, crystal orientation of electrode surface and crystallographic lattice of the crystalline deposit-substrate [1].

For the first time, nanostructure metals and alloys were prepared by blowing inert metallic gas on a cold substrate in which fast gas condensation and fast nucleation occurred; thus, nanometric grain sizes were obtained. Among other methods, plasma, physical and chemical vapour deposition, electrochemical deposition, fast solidification, mechanical alloying and severe plastic deformation can be numerated. Nanostructures prepared by electrodeposition, however, have been widely investigated since 1990 [1].

Recently, studies are done on nanocomposite coatings prepared by electrodeposition method. These coatings due to their high corrosion and wear resistance, have a wide range of applications in automobile industry, engines and casting modules [2]. Theoretical model for electrodeposition process of metal matrix composite can be delineated into

four stages: (1) surface charge formation on the particle surface of the suspension, (2) mass transfer of particles from the suspension onto the cathode surface, (3) the interaction between cathode surface and particles and (4) nanoparticles entrapped in the growing metal layers [3].

Electrochemical deposition can be achieved by direct current (DC), pulse current (PC) [4], pulse reverse current (PRC) and pulse potentiostatic deposition [3]. In DC method, the current remains stable with respect to time, while in PC method, the current at T_{ON} (ON time) has a certain value, but at T_{OFF} (OFF time) it is zero [4]. In PRC method, the current has a positive value at T_{ON} and a negative value at T_{OFF} [3].

It should be mentioned that there are two important parameters in pulse current method: pulse frequency and duty cycle. Pulse frequency is obtained from the following equation:

$$F = 1/(T_{ON} + T_{OFF}). \quad (1)$$

While the duty cycle can be obtained from:

$$\gamma = T_{ON}/(T_{ON} + T_{OFF}). \quad (2)$$

In DC method, the duty cycle is always 100% [5].

Different studies demonstrated that by increasing the current density, microhardness of coated layer decreases [2,6–19]. Accordingly, current density has an optimum value for nanocomposite coating in electrodeposition process. Yang and

* Author for correspondence (s.imanian.sut@gmail.com)

Cheng [5] reported that in manufacturing Ni–Co/SiC nanocomposite coating, by increasing the pulse frequency and reducing duty cycle, SiC content in the coating increased, thereby the microhardness of coated film increased. Microhardness of coating which was prepared in PRC method is more than that of in PC method. Also in PC method, microhardness of prepared coating is more than that of in DC method [4].

Arunsunai Kumar *et al* [20] concluded that in generating Ni–W/TiO₂ coating, micro hardness of prepared coating in PC method was more than that in DC method. Shahri and Allahkaram [8] reported that in preparing Co/BN nanocomposite coating, by increasing the current density to a specific value, grain size decreased which is due to the increase in nucleation rate. But further increasing the current density, because of changes in both surface energy and growth mechanisms in the presence of hydrogen, grain size increased. Yang and Cheng [5] reported that increasing the pulse frequency and decreasing the duty cycle led to increase in the amount of particles in the Ni–Co/SiC composite coating, thereby grain size reduces. Many studies have concentrated on the effective parameters in preparing nickel-based nanocomposite coatings.

During the preparation of Ni/CeO₂ nanocomposite coating, Sen *et al* [21] found that by increasing the temperature, kinetic and thermodynamic driving forces affect the final grain size of Ni/CeO₂ nanocomposite coating. In another study, effect of uniform distribution on the nickel matrix was evaluated and it was concluded that TiO₂ nanoparticles could restrain the growth of nickel grains [11]. Another study concluded that adding SiC nanoparticles could limit crystalline growth of deposited zinc metal [14]. Effect of adding SiC nanoparticles was also investigated in another study [22]. It was found that the nanoparticles by reducing the mobility of grain boundaries of nickel (pinning effect), led to reduction of the grain growth of nickel.

Arab Juneghani *et al* [16] reported that the addition of SiC nanoparticles led to increase in the number of nucleation sites in the matrix and thereby the grain size decreased. Also, the addition of Si₃N₄ nanoparticles into the copper matrix, leads to decrease in the grain size of prepared nanocomposite coating [17,23]. In another research, grain size of Ni–Fe₂O₃ nanocomposite coating was finer than pure nickel coating [24]. Addition of nanoparticles to the plating bath and their entrapment in the nickel matrix caused to reduce the grain size of nanocomposite coating [7,20,25–35]. Finally, during preparing Ni–W–B/CeO₂ nanocomposite coating, Wang Junli *et al* [36] concluded that decreasing duty cycle from 75 to 10% led to decrease the grain size.

No study has yet focussed on Ni–Co/SiO₂ nanocomposite coating prepared by electrodeposition method. In the present work, for the first time, Ni–Co nanocomposite coating reinforced by SiO₂ nanoparticles was processed by electrodeposition method and effects of electrodeposition parameters such as average current density, pulse frequency and duty cycle on microhardness and grain size of nanocomposite coating were investigated. There were insufficient reports

about effect of current density, pulse frequency and duty cycle on the microhardness and grain size of the coating. Analysis of previous works were merely an observation and are reported. According to the nature of these phenomena, comprehensive and novel analyses are presented here. Also, the effects of electrodeposition methods (PC and DC), current density, pulse frequency and duty cycle on the surface morphology of coatings have never been investigated before.

2. Materials and methods

Ni–Co coating and Ni–Co/SiO₂ nanocomposite coating were deposited on the substrate of a 1 × 1 cm mild carbon steel (with 0.43% carbon) by direct and pulse current methods. The carbon steel substrates as cathode were polished by emery paper (400, 600 and 1000) prior to the electrodeposition process and then dipped in ethanol and 10% HCl for 2 min and 15 s, respectively. Finally, the substrates were washed in distilled water. A sheet of pure 1 × 1 cm nickel was used as anode.

Working surface area of all the samples was 1 and 3 cm² for cathode and anode, respectively. Pulse and direct current were produced by a power supply. The electrolyte was agitated via a digital magnetic stirrer with a hot plate. Coating bath volume was 100 ml and the length of magnet was 2 cm. As shown in table 1, Watt's bath composition was used to prepare the electrolyte for coating. In this work, 20 nm SiO₂ nanoparticles (99.5% Merck) were used as reinforcement. Eleven specimens were coated by Ni–Co/SiO₂ nanocomposite. Also two Ni–Co alloy-coated samples were prepared.

Table 2 reports the electrodeposition parameters for preparing the specimens. Variations of current density from 2 to 4 and 6 to 8 A dm^{−2} are applied on specimens 1–4.

Samples 5, 2, 6 and 7 show variations of pulse frequency from 5 to 10 and 25 to 100 Hz. Specimens 8, 9, 2 and 10 represent variations of duty cycles from 30 to 40 and 50 to 60%.

Conditions for preparing the samples are as follows: 50°C electrolyte temperature, 300 rpm stirring rate, 4.3 pH and 90 min coating time. For all the electrolytes, 50 ml distilled water with SiO₂ nanoparticles and sodium dodecylsulphate (98% Scharlou) were primarily added to the beaker and agitated for 24 h at a stirring rate of 1200 rpm. Watt's materials and distilled water were respectively added to the beaker until water volume reached to 100 ml. When the coating solution was prepared, temperature of magnetic stirrer plate was increased until the solution temperature reached to 50°C.

Table 1. Composition of the plating bath.

Material	Concentration (g l ^{−1})
NiSO ₄ ·6H ₂ O	220
NiCl ₂ ·6H ₂ O	40
H ₃ BO ₃	30
CoSO ₄ ·7H ₂ O	25
nano-SiO ₂	15
Sodium dodecylsulphate	0.3

Table 2. Electrodeposition parameters for preparing the specimens.

Specimen number	Current type	Current density (A dm ⁻²)	Pulse frequency (Hz)	Duty cycle (%)
(Ni–Co/SiO ₂), 1	Pulse	2	10	50
(Ni–Co/SiO ₂), 2	Pulse	4	10	50
(Ni–Co/SiO ₂), 3	Pulse	6	10	50
(Ni–Co/SiO ₂), 4	Pulse	8	10	50
(Ni–Co/SiO ₂), 5	Pulse	4	5	50
(Ni–Co/SiO ₂), 6	Pulse	4	25	50
(Ni–Co/SiO ₂), 7	Pulse	4	100	50
(Ni–Co/SiO ₂), 8	Pulse	4	10	30
(Ni–Co/SiO ₂), 9	Pulse	4	10	40
(Ni–Co/SiO ₂), 10	Pulse	4	10	60
(Ni–Co/SiO ₂), 11	Direct	4	–	100
(Ni–Co), 12	Pulse	4	10	50
(Ni–Co), 13	Direct	4	–	100

Electrolyte metallic salts such as NiSO₄·6H₂O and CoSO₄·7H₂O were dissolved in water and subsequently dissociated into positive and negative ions. Because of high surface activity of nanoparticles, positive ions (Ni²⁺ and Co²⁺) stuck on the surface of nanoparticles and formed an positive ionic cloud around them. This led to the attraction of nanoparticles by cathode surface, so that they entrapped into the matrix and nanocomposite was formed.

Owing to characterization, Buhler microhardness device was employed to determine Vickers microhardness. Tests were done under vertical load of 100 g and loading time of 10 s. The microhardness of each sample was measured 10 times and the average value was chosen as microhardness of specimen. To investigate the phase structure of the specimens, X-ray diffraction (stoe-stadi-mp) with a CuK α radiation of 0.154 nm wave length was used. Moreover, surface morphology, elemental analysis and elemental distribution were investigated through field emission scanning electron microscope (FESEM MIRA 3 TESCAN).

Energy dispersive X-ray spectroscopy (EDX) and X-ray map (which attached to the FESEM) were employed to investigate elemental analysis and elemental distribution of coatings, respectively. Grain size of Ni–Co/SiO₂ nanocomposite coating was calculated through famous Scherrer's equation (equation (3)):

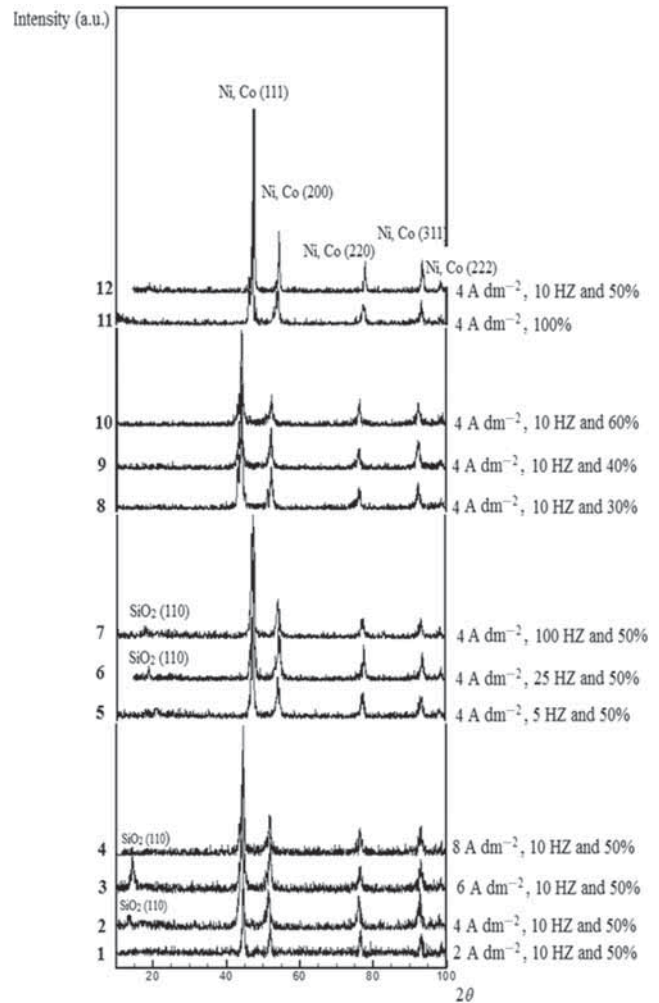
$$t = 0.9\lambda / B \cos \theta_B, \quad (3)$$

where t is the grain size in nanometers, λ the wavelength (0.154 nm) of CuK α radiation, B the full width half maximum (FWHM) at $2\theta_B$ radians and θ_B the Bragg's angle [37].

3. Results and discussion

3.1 Phase structure

Figure 1 illustrates X-ray diffraction patterns for 12 specimens obtained by changing current density, pulse frequency

**Figure 1.** X-ray diffraction patterns in different electrodeposition conditions of coatings extracted from table 2.

and duty cycle for Ni–Co/SiO₂ nanocomposite coatings and Ni–Co alloy coatings prepared by pulse current electrodeposition method. In this figure, the number of XRD patterns are related to the number of samples in table 2. Production conditions have been described in table 2. Peaks related to nickel–cobalt alloy were observed in $2\theta = 45, 51.5, 76.3, 93$ and 98.5° . Moreover, SiO₂-related peak (plane of (110) in $2\theta = 14^\circ$) could be seen in just four of the specimens with higher microhardness and abundant amount of entrapped SiO₂ nanoparticles.

In these patterns, peaks of nickel–cobalt alloy and their related plane can be observed. Related ranges of nickel–cobalt alloy peaks were as follows: (40–50°), (50–60°), (70–80°) and (90–100°). All the specimens exhibited the growth orientation of crystal face (111). Because plane (111) had the most diffraction intensity. The addition of SiO₂ nanoparticles had no effect on the intensity.

In another research to prepare Ni–Co–TiO₂ nanocomposite coating by pulse electrodeposition method on a mild steel substrate it was reported that for Ni–Co without TiO₂ nanoparticles, plane (200) (with maximum intensity) was

dominant for crystal growth orientation, but by adding 2.5 wt% of TiO₂ nanoparticles into the coating, the orientation of the composite coatings changed from (200) to (111) (with maximum intensity) [35].

Differences between the researches are maybe due to different electrodeposition parameters such as temperature, stirring rate, plating time, pH, type of nanoparticles and chemical composition of plating bath. All of these parameters are very prominent and could impress the coating process. Other crystal planes related to nickel–cobalt alloy were (200), (220), (311) and (222).

If the wt% of some phases in a sample is less than the critical value (it depends on accuracy of XRD device, type of phase and matrix), XRD device cannot show their related peaks, or the intensity of the peaks will be too low to see and can be ignored. Maybe because of the mentioned reasons, in some specimens, amount of SiO₂ nanoparticles was too low and SiO₂-related peak had been disappeared. With regards to XRD analysis and diagrams of microhardness of coatings, it becomes clear that specimen with the sharpest SiO₂ peak (see figure 1, specimens number 3), has the most microhardness, too (see figure 5b, microhardness corresponds to the current density of 6 A dm⁻²). Also, it has the sharpest SiO₂ and Si-related peaks in XRD and EDX results, respectively.

These results can be investigated and generalized to other specimens.

The prominent Bragg's law as follows:

$$n\lambda = 2d_{hkl} \sin \theta, \quad (4)$$

where n is the order of reflection, which may be any integer (1, 2, 3, ...), λ the X-ray wavelength, d_{hkl} the inter planar separation for a plane having indices h , k and l and θ the angle of diffraction for constructive interference. Distance between two adjacent and parallel planes of atoms for a cubic crystal is as follows:

$$d_{hkl} = a/\sqrt{h^2 + k^2 + l^2}. \quad (5)$$

Here a is the lattice parameter.

From these two recent equations, it is obvious that there is an inverse relationship between θ and d_{hkl} . It means that by increasing each one, the other one is decreased. Tensile and compressive strains can increase and decrease the d_{hkl} value; thus, can shift the peaks to the right and left, respectively [37].

According to figure 1, remarkable shifts in XRD patterns of some specimens have been created. This phenomena refer to the amount and type of strain that can be tensile or

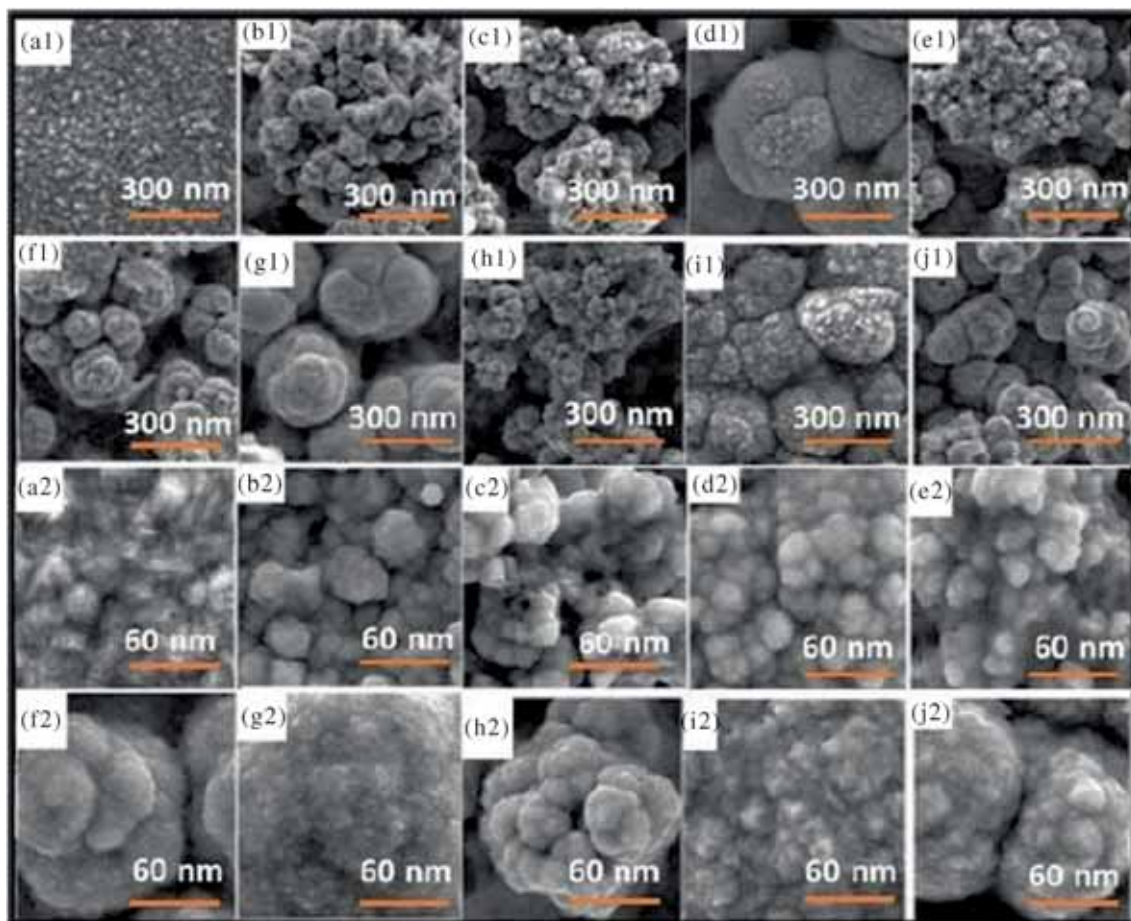


Figure 2. FE-SEM images of coatings, DET: secondary electron, average SEM HV: 15 kV, average work distance: 13.6 mm.

compressive. Ni–Co/SiO₂ is a nickel-based nanocomposite. It is known that lattice parameters of nickel and cobalt are about 0.35 and 0.25 nm, respectively. Formation of solid solution between nickel and cobalt because of less amount of lattice parameter of cobalt caused tensile strain in nickel lattice (right shift). However, by adding SiO₂ nanoparticles, compressive strain can be made on the coating (left shift). So the amount of cobalt and SiO₂ nanoparticles in the coating determined the amount and type of strain. In figure 1, it can be seen that XRD pattern of specimen 12 (Ni–Co alloy coating without SiO₂ nanoparticles) has the most shift to the right. By adding SiO₂ nanoparticles into the coating (especially in specimens 1, 2, 3, 4, 8, 9 and 10), it can be seen that patterns shift to the left. In other specimens (5, 6, 7 and 11) because of heterogeneous distribution of cobalt and SiO₂ on the coating all or portion of tensile and compressive strains neutralized each other. Maybe XRD analysis prepared from the zones of coatings which the aggregation of cobalt is much higher

than that of SiO₂ nanoparticles. So generally, there was low compressive strain in those places of coating; thus, low shift (to left) in the XRD results could be seen.

3.2 FESEM images, X-ray map and EDX analysis of Ni–Co/SiO₂ nanocomposite coating

Figure 2 indicates FESEM images of Ni–Co/SiO₂ nanocomposite coating. To investigate effect of pulse frequency, current density and duty cycle on the morphology of samples, a comparison was done between samples produced in the lowest (5 Hz) and the highest (100 Hz) values of pulse frequency. Also, samples with minimum (2 A dm⁻²) and maximum (8 A dm⁻²) values of current density and duty cycle (minimum 30% and maximum 60%, respectively) were compared. The reason for these selections was to create the greatest differences between coating morphologies via the most variation range of mentioned parameters.

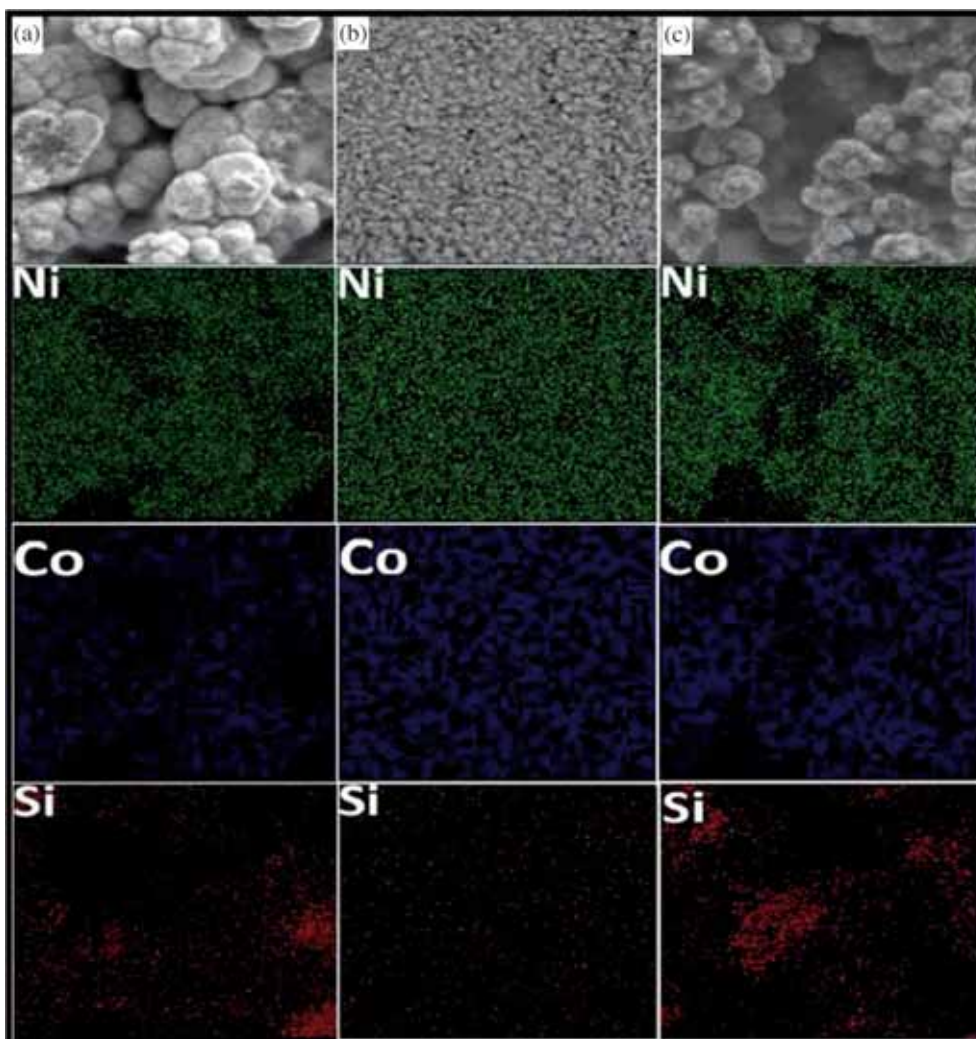


Figure 3. Ni–Co/SiO₂ nanocomposite coating, X-ray map, Ni, Co and Si distribution, magnification 10000. (a) Pulse current type, current density 6 A dm⁻², pulse frequency 10 Hz, duty cycle 50%, (b) pulse current type, current density 4 A dm⁻², pulse frequency 10 Hz, duty cycle 50%, (c) pulse current type, current density 4 A dm⁻², pulse frequency 25 Hz, duty cycle 50%.

Also, morphology of samples which have been produced under pulse and direct current electrodeposition methods (conditions, in pulse current method: 4 A dm⁻², 10 Hz and 50% and in direct current method: 4 A dm⁻², 100%, respectively) were compared. So, among these 13 specimens, totally 10 specimens were selected to investigate the surface morphology. Here, samples have been introduced from a1 to j2. It should be mentioned that samples with same english alphabet belong to one sample. For example, a1 and a2 are related to one. Sample indexes 1 and 2 refer to the magnification of 10,000 and 50,000, respectively.

As a result of long T_{ON} and T_{OFF} , the discharge rate in low pulse frequency (c1 and c2 images, conditions: 4 A dm⁻², 5 Hz and 50%) is more than that of high pulse frequency (d1 and d2 images, conditions: 4 A dm⁻², 100 Hz and 50%). At high current densities (h1 and h2 images, conditions: 8 A dm⁻², 10 Hz and 50%) and high duty cycles (e1 and e2 images, conditions: 4 A dm⁻², 10 Hz and 60%), the discharge rate increases. Conversely, at low current densities (g1 and g2 images, conditions: 2 A dm⁻², 10 Hz and 50%) and low duty cycles (f1 and f2 images, conditions: 4 A dm⁻², 10 Hz and 30%), the rate is reduced. Therefore,

in low discharge rates (like low solidification rates), the surface morphology is ordered, smooth and gross globular, while in high discharge rates (like high solidification rates), the surface morphology is disordered, rough and fine globular. FESEM images of Ni-Co/SiO₂ nanocomposite coatings that were prepared by pulse current (a1 and a2 images, conditions: 4 A dm⁻², 19 Hz and 50%) and direct current (b1 and b2 images, conditions: 4 A dm⁻² and 100%) were shown. It can be seen that in pulse current method, surface morphology is smoother and more ordered, yet in direct current method, surface structure is rough, disordered and gross globular. In direct current method, discharge rate is more than that of produced in pulse current method. As a result, in pulse current method, the surface morphology is same as the low solidification rate structure. In direct current method, however, the surface morphology is similar to high solidification rate structure, yet it is rough and disordered.

By comparing FESEM images of Ni-Co alloy coatings prepared by pulse current (i1 and i2 images, conditions: 4 A dm⁻², 10 Hz and 50%) and direct current (j1 and j2 images, conditions: 4 A dm⁻² and 100%), due to the high discharge rate of direct current, the surface morphology is

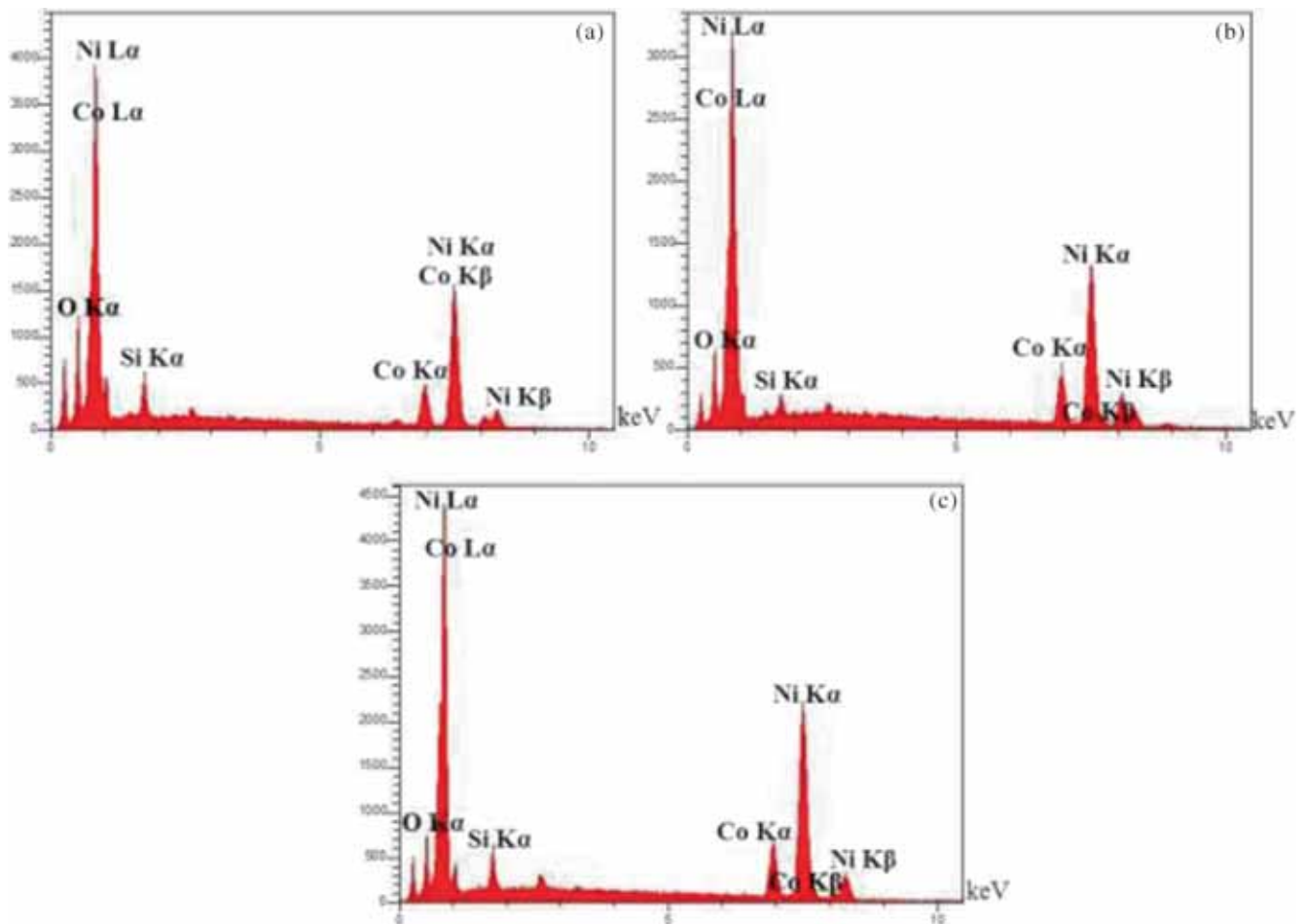


Figure 4. EDX analysis of Ni-Co/SiO₂ nanocomposite coating; (a) pulse current type, current density 6 A dm⁻², pulse frequency 10 Hz, duty cycle 50%, (b) pulse current type, current density 4 A dm⁻², pulse frequency 10 Hz, duty cycle 50%, (c) pulse current type, current density 4 A dm⁻², pulse frequency 25 Hz, duty cycle 50%.

rough, disordered and gross globular. Nonetheless, in pulse current surface, the morphology is smoother, more ordered and fine globular. According to figure 2, it is obvious that surface morphologies are almost similar in some samples like b1: direct current, c1: minimum pulse frequency and e1: maximum duty cycle. This is because, under these conditions precipitation rate of coatings was high. In these situations like high solidification rate, the surface morphology was rougher, more disordered and gross globular.

Also, there is no major difference between f1: minimum duty cycle and e1: maximum duty cycle. Actually, duty cycle changed from 30 to 60%. It means that duty cycle has been redoubled. Current density (variation from 2 to 8 A dm⁻²) has been quadruplicated. Maximum value of pulse frequency (100 Hz) is 20 times more than the minimum value (5 Hz). It can be said that variation of duty cycle in comparison to other electrodeposition parameters was so less. This is the reason for low change in surface morphology of coating via variation in duty cycle.

Figure 3 delineates the X-ray map (which attached to FESEM) of three Ni-Co/SiO₂ nanocomposite coating specimens where Ni, Co and Si distributions are clearly seen in the matrix. Ni and Co are distributed homogeneously in prepared Ni-Co alloy. Also, it can be seen that Si (refer to SiO₂

nanoparticles) is distributed in matrix (Ni-Co alloy) and this confirms that Ni-Co/SiO₂ nanocomposite coating has been prepared successfully. Figure 4 displays EDX analysis (which attached to FESEM) of three Ni-Co/SiO₂ nanocomposite coating specimens. This figure represents that presence of Ni, Co, O and Si elements in the coating caused the formation of Ni-Co/SiO₂ nanocomposite coating. Table 3 shows the EDX analysis of the wt% of Ni, Co and Si elements and SiO₂ nanoparticles in Ni-Co/SiO₂ nanocomposite coating.

3.3 Effect of average current density on the grain size and microhardness of Ni-Co/SiO₂ nanocomposite coating

Figure 5a shows grain size variations of Ni-Co/SiO₂ nanocomposite coating by increasing (average) the current density. By increasing the average current density from 2 to 6 (A dm⁻²), grain size decreased, but with further increasing to 8 (A dm⁻²), the grain size increased. Through increasing the nanoparticles in the coating, grain size decreased since entrapped nanoparticles have more influence on the grain size of Ni-Co/SiO₂ nanocomposite coating. Increasing the amount of these nanoparticles in the coating, decreases the grain size, because these nanoparticles could decrease grain boundary mobility and prevent grain growth, and also nanoparticles are suitable places for heterogeneous nucleation [10].

For low-average current density, electrodeposition process did not complete properly, because attraction forces between the surrounded nanoparticles by positive metallic ions and cathode surface were weak. But in high current density, chances for reduction of independent positive ions (Ni²⁺ and Co²⁺) were more than nanoparticles (with cationic cloud around them). So, the nanoparticles entrapment was limited. Therefore, there was an optimum average current density value.

Figure 5b illustrates the variations of microhardness of nanocomposite by increasing the (average) current density. As can be seen with the increase in the average current

Table 3. EDX analysis of wt% of Ni, Co and Si elements and SiO₂ nanoparticles in Ni-Co/SiO₂ nanocomposite coating. (a) Pulse current type, current density 6 A dm⁻², pulse frequency 10 Hz, duty cycle 50%. (b) Pulse current type, current density 4 A dm⁻², pulse frequency 10 Hz, duty cycle 50%. (c) Pulse current type, current density 4 A dm⁻², pulse frequency 25 Hz, duty cycle 50%.

Material/specimens	Ni (wt%)	Co (wt%)	Si (wt%)	SiO ₂ (wt%)
a	67.68	14.98	2.78	6.65
b	74.67	12.76	1.49	3.19
c	76.12	15.80	1.91	4.08

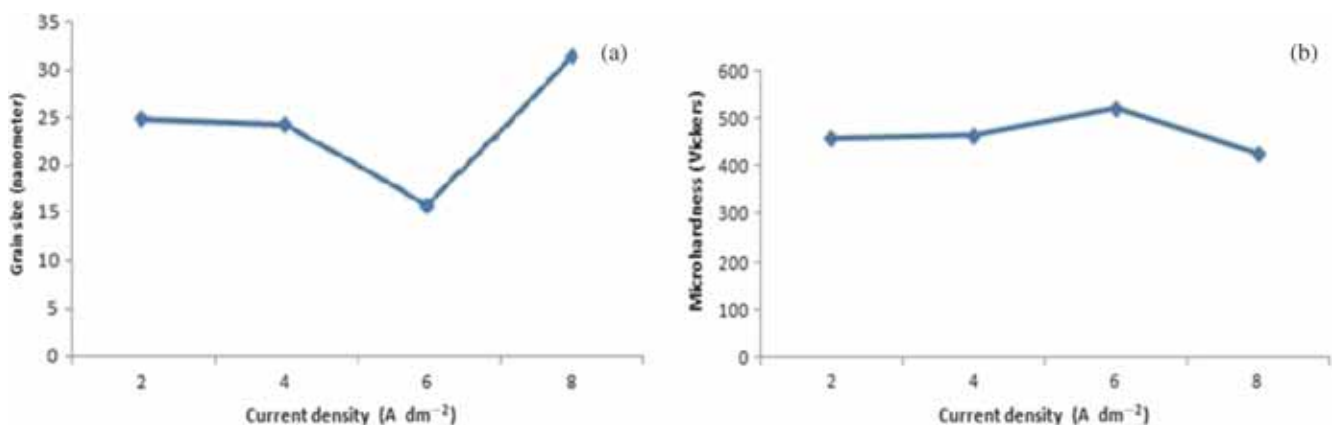


Figure 5. (a) Effect of current density variations on the Ni-Co/SiO₂ nanocomposite coating grain size, pulse frequency 10 Hz, duty cycle 50%. (b) Ni-Co/SiO₂ nanocomposite coating microhardness variations with current density variations in pulse frequency of 10 Hz and duty cycle of 50%.

density from 2 to 6 (A dm^{-2}), the microhardness coating increased, but by further increasing the average current density, it decreased. In low current density, because of the low electrical charge, the attraction between nanoparticles surrounded by positive ion clouds and cathode is low. So the hydrodynamic forces which were caused by electrolyte agitation could dislodge nanoparticles, which were wickedly attracted by the substrate from the cathode surface. That is why nanoparticles content in the coating decreased and consequently, microhardness is reduced. By increasing the average current density to 6 (A dm^{-2}), the attraction force between nanoparticles (which were surrounded by cationic cloud) and cathode increased. Consequently, the amount of nanoparticles in the coating increased and thereby the microhardness has been increased. However, by further increasing the average current density to 8 (A dm^{-2}), independent positive nickel and cobalt ions were attracted to the substrate more than nanoparticles (surrounded by positive ion cloud). Also, the number of nanoparticles surrounded by positive ion cloud in electrolyte is decreased, subsequently amount of nanoparticles in the coating decreased which led to the reduction of microhardness.

Such as the other research [6] in manufacturing another nanocomposite coating, it can be concluded that optimum average current density for preparing Ni-Co/SiO₂ nanocomposite coating was 6 (A dm^{-2}).

3.4 Effect of pulse frequency on the grain size and microhardness of Ni-Co/SiO₂ nanocomposite coating

Figure 6a shows variation in grain size of Ni-Co/SiO₂ nanocomposite coating by increasing pulse frequency. In direct current method, the current is always on, the process is fast and mostly positive metallic ions are reduced. On the contrary, the process is slower in pulse current method due to the presence of T_{ON} and T_{OFF} . In the OFF times, there were more chances for nanoparticles to be surrounded by positive ion clouds and then reach the cathode surface using agitation forces and finally in ON times, they can be discharged there. In low pulse frequencies, T_{OFF} and T_{ON} are

so high. Because of very high T_{OFF} , attraction force between surrounded nanoparticles and cathode were so weak. Also because of very high T_{ON} , independent positive metallic ions were discharged much faster than surrounded nanoparticles. So in low pulse frequencies, grain size was increased. By increasing the pulse frequency to an optimum value (25 Hz), because of T_{ON} and T_{OFF} decrease, the amount of nanoparticles in the coating increased, thereby grain size reduced.

In high pulse frequencies, T_{ON} and T_{OFF} were very short and the chance for SiO₂ nanoparticles to be surrounded by positive ions is low. Accordingly, for low (less than 25 Hz) and high (more than 25 Hz) pulse frequencies, the amount of nanoparticles in the coating were decreased, thereby grain size of coating was increased.

Figure 6b represents the influence of pulse frequency on the Ni-Co/SiO₂ nanocomposite coating microhardness. As it is shown, by increasing the pulse frequency from 5 to 25 Hz, microhardness increased, but by further increasing from 25 to 100 Hz, it decreased. In low pulse frequency, T_{ON} and T_{OFF} are too long and hydrodynamic forces could dislodge nanoparticles surrounded by positive ion cloud from the cathode surface, hence, the content of nanoparticles in the coating decreased, so microhardness of sample reduced.

On the other hand, T_{OFF} was more than optimum value and the amount of nanoparticles surrounded by positive ion cloud increased in the electrolyte, but since T_{OFF} was too long, they could not be attracted by substrate. T_{ON} was also very long and the metal positive ions were quickly attracted to the substrate; thus, amount of nanoparticles in the coating were decreased, followed by decreasing the microhardness of samples. By increasing the pulse frequency this problem can be solved, it means that T_{ON} and T_{OFF} can get closer to the optimum value, hence, the amount of nanoparticles in the coating were increased. Nonetheless, with further increase in the pulse frequency from 25 to 100 Hz, T_{ON} and T_{OFF} become short. T_{OFF} for nanoparticles surrounded by metal positive ion cloud was less than optimum value, thereby amount of nanoparticles in the coating and microhardness were decreased. As mentioned in other researches [11,22],

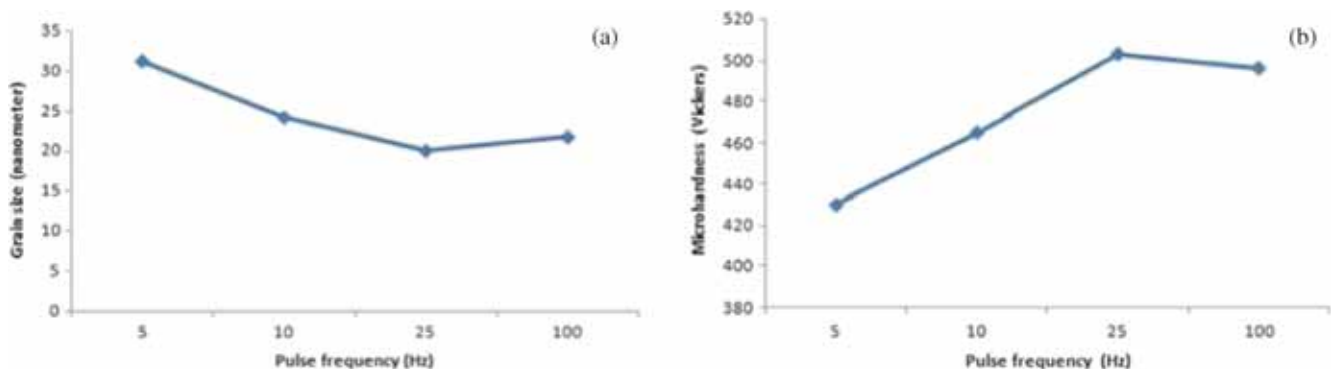


Figure 6. (a) Ni-Co/SiO₂ nanocomposite coating grain size variation with increasing pulse frequency, current density 4 A dm^{-2} , duty cycle 50%. (b) Influence of pulse frequency on the Ni-Co/SiO₂ nanocomposite coating microhardness in current density of 4 A dm^{-2} and duty cycle of 50%.

there is an optimum value for pulse frequency in preparing other nanocomposite coatings. In this work, for preparing Ni-Co/SiO₂ nanocomposite coating, optimum value of pulse frequency (to get maximum microhardness) was 25 Hz.

3.5 Effect of duty cycle on the grain size and microhardness of Ni-Co/SiO₂ nanocomposite coating

Figure 7a shows variations in grain size of Ni-Co/SiO₂ nanocomposite coating by increasing the duty cycle. In low duty cycle values (less than 50%), T_{OFF} is very long; on the contrary, T_{ON} is so short and the conditions are the same as those of in low current density. However, in high duty cycle values (more than 50%), T_{OFF} is very short, but T_{ON} is very long and the conditions are the same as high current density values. Moreover, it can be seen that in duty cycle of 100% (direct current electrodeposition method), grain size of Ni-Co/SiO₂ nanocomposite coating is greater than that of in pulse current electrodeposition method.

It is expected that by reducing the duty cycle and increasing the amount of nanoparticles in the coating, grain size of nanocomposite coating was decreased [5].

Figure 7b shows the Ni-Co/SiO₂ nanocomposite coating microhardness changes caused by duty cycle variations. As can be observed, in low duty cycles, T_{OFF} is too long, attraction force between substrate and nanoparticles surrounded by metal positive ion cloud is so weak that the hydrodynamic

forces could dislodge the nanoparticles from the substrate surface. Consequently, reducing the amount of nanoparticles in the coating caused the reduction in microhardness.

By increasing the duty cycle to 50%, because T_{OFF} is shorter, mentioned problems disappeared. So, the amount of nanoparticles in the coating and microhardness were increased. However, by further increasing the duty cycle to 100% (DC method), T_{ON} becomes so long, and mostly metal positive ions were more fortunate to achieve the cathode. Also, the quantity of nanoparticles surrounded by metal positive ion cloud declined in the solution. Therefore, the amount of nanoparticles in the coating and the microhardness were decreased. Thus, duty cycle has an optimum value [14,22], which for preparing Ni-Co/SiO₂ nanocomposite was 50%. As can be seen, coating microhardness in direct current method (100% of duty cycle) was less than that of in pulse current method.

Figure 8 provides a comparative image between the grain sizes of different kinds of coating. It can be seen that nanocomposite coating has a finer grain size than alloy coating (since nanocomposite coating involves nanoparticle reinforcements) and in direct current method greater grain sizes can be reached.

In figure 9, the microhardness of some coatings prepared by pulse and direct methods and steel substrate are compared. Results showed that nanocomposite coating had better microhardness than alloy coating and this microhardness was higher when pulse current method was used. It can be explained by the fact that in pulse method, there are OFF times and ON times. Perhaps because of OFF times and thereby less rate of process, there were more chance and time for nanoparticles which are surrounded by positive ions (Ni²⁺ and Co²⁺) and then move to the cathode surface and

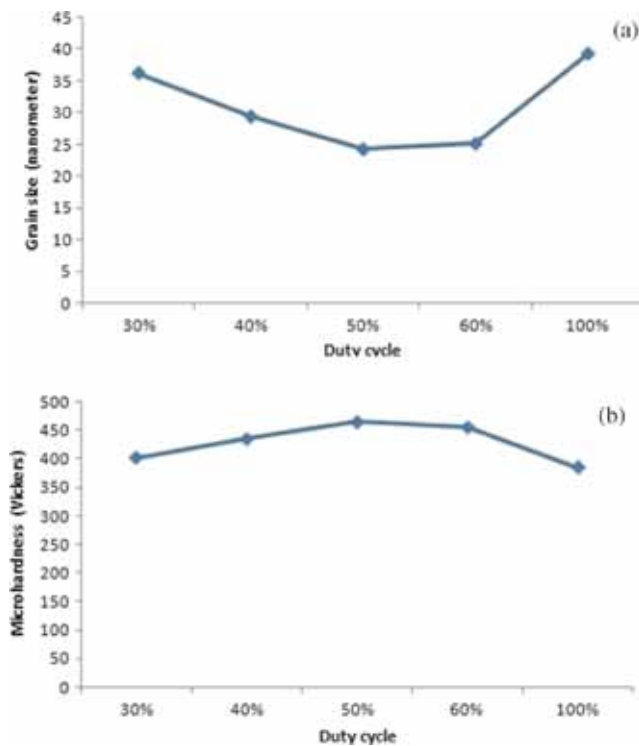


Figure 7. (a) The influence of duty cycle percent on the Ni-Co/SiO₂ nanocomposite coating grain size, current density 4 A dm⁻², pulse frequency 10 Hz. (b) The effect of duty cycle variations on the Ni-Co/SiO₂ nanocomposite coating microhardness in current density of 4 A dm⁻² and pulse frequency of 10 Hz.

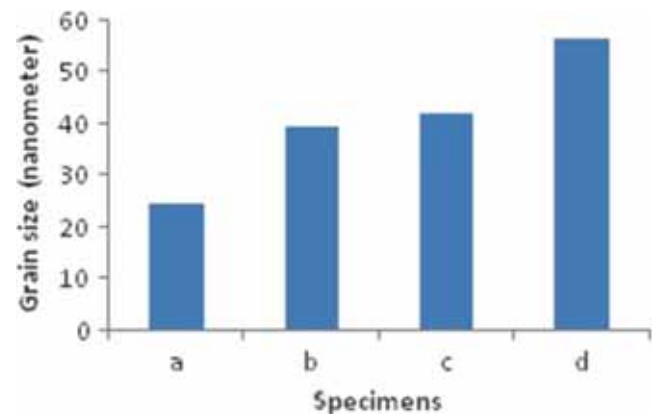


Figure 8. Comparison of grain size between (a) Ni-Co/SiO₂ nanocomposite coating prepared in pulse current electrodeposition method, current density of 4 A dm⁻², pulse frequency of 10 Hz, duty cycle of 50%. (b) Ni-Co/SiO₂ nanocomposite coating prepared in direct current electrodeposition method, current density of 4 A dm⁻². (c) Ni-Co alloy coating prepared in pulse current electrodeposition method, current density of 4 A dm⁻², pulse frequency of 10 Hz, duty cycle of 50%. (d) Ni-Co alloy coating prepared in direct current electrodeposition method, current density of 4 A dm⁻².

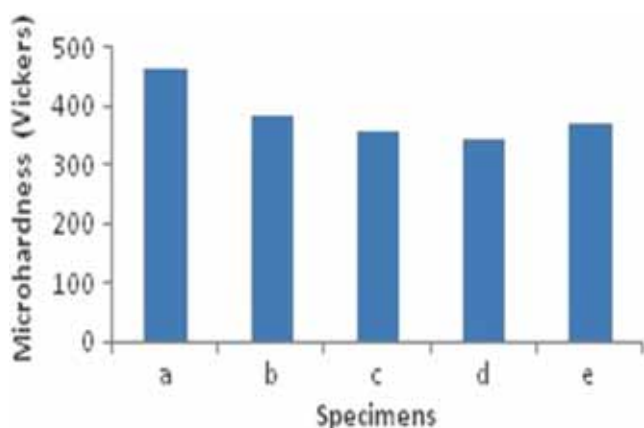


Figure 9. Comparison of microhardness between (a) Ni–Co/SiO₂ nanocomposite coating prepared in pulse current electrodeposition method, current density of 4 A dm⁻², pulse frequency of 10 Hz, duty cycle of 50%. (b) Ni–Co/SiO₂ nanocomposite coating prepared in direct current electrodeposition method, current density of 4 A dm⁻². (c) Ni–Co alloy coating prepared in pulse current electrodeposition method, current density of 4 A dm⁻², pulse frequency of 10 Hz, duty cycle of 50%. (d) Ni–Co alloy coating prepared in direct current electrodeposition method, current density of 4 A dm⁻². (e) Steel substrate.

would be reduced there. But in direct current method, the rate of coating increased. So, there was more chance for Ni²⁺ and Co²⁺ to be reduced on the cathode surface, so the amount of surrounded nanoparticles by positive ions was decreased and consequently, the amount of entrapped nanoparticles in the coating lessened and thereby microhardness was reduced.

Finally in table 3, elemental distribution and analysis for three samples which have maximum microhardness and minimum grain size have been indicated. Here, samples a, b and c are samples 3, 2 and 6 in table 2, respectively.

4. Conclusions

In general, in this study, Ni–Co/SiO₂ nanocomposite coating was prepared by electrodeposition method for the first time. Effects of average current density, pulse frequency and duty cycle on the microhardness, grain size and surface morphology of the coating were also investigated. The microhardness, grain size and surface morphology of Ni–Co alloy and Ni–Co/SiO₂ nanocomposite coating that were prepared in the DC and PC methods have also been compared.

In high discharge rates (high current density, duty cycle, low pulse frequency and DC method), the surface morphology was rough, disordered and gross globular, conversely in low discharge rates (low current density, duty cycle, high pulse frequency and PC method), it was smoother, more ordered and fine globular.

Results indicated that in DC method, grain size of coating was higher than that of in the PC method. Also, grain size in Ni–Co/SiO₂ nanocomposite coating was less than that in Ni–Co alloy coating.

Additionally, the microhardness of coatings produced by PC method was more than that of in DC method. Furthermore, the microhardness of Ni–Co/SiO₂ nanocomposite coating was more than Ni–Co alloy coating.

For average current density, duty cycle and pulse frequency, there were optimum values (6 A dm⁻², 50% and 25 Hz, respectively) and any deviation from those optimum values led to increase in the grain size, while decrease in the microhardness.

It was concluded that SiO₂ nanoparticles entrapped in the coating, influenced on the grain size and microhardness of Ni–Co/SiO₂ nanocomposite coating. It means that when the amount of nanoparticles in the coating increased, the coating grain size decreased but microhardness increased.

Acknowledgement

We are thankful to the Advanced Materials and Nanotechnology Research Laboratory, Faculty of Materials Science and Engineering, K N Toosi University of Technology, for supporting this work.

References

- [1] Gurrappa I and Binder L 2008 *Sci. Technol. Adv. Mater.* **9** 043001
- [2] Srivastava M, William Grips V K and Rajam K S 2007 *Appl. Surf. Sci.* **253** 3814
- [3] Gomes A, Pereira I, Fernández B and Pereiro R 2011 *Electrodeposition of metal matrix nanocomposites: improvement of the chemical characterization techniques, in Advances in nanocomposites—synthesis, characterization and industrial applications* (ed) Boreddy Reddy ISBN: 978-953-307-165-7, InTech
- [4] Devaraj G et al 1990 *Mater. Chem. Phys.* **25** 439
- [5] Yang Y and Cheng Y F 2013 *Surf. Coat. Technol.* **216** 282
- [6] Bagheri P, Farzam M, Mousavi A B and Hosseini M 2010 *Surf. Coat. Technol.* **204** 3804
- [7] Vaezi M R, Ssadrnezhzaad S K and Nikzad L 2008 *Colloids Surf. A* **315** 176
- [8] Shahri Z and Allahkaram S R 2012 *Iranian J. Mater. Sci. Eng.* **9** 1
- [9] Yao Y, Yao S, Zhang L and Wang H 2007 *Mater. Lett.* **61** 67
- [10] Karbasi M, Yazdian N and Vahidian A 2012 *Surf. Coat. Technol.* **207** 587
- [11] Lajevardi S A and Shahrabi T 2010 *Appl. Surf. Sci.* **256** 6775
- [12] Singh D K and Singh V B 2012 *Mater. Sci. Eng. A* **532** 493
- [13] Pouladi S, Shariat M H and Bahrololoom M E 2012 *Surf. Coat. Technol.* **213** 33
- [14] Sajjadnejad M, Mozafari A, Omidvar H and Javanbakht M 2014 *Appl. Surf. Sci.* **300** 1
- [15] Ozkan S et al 2013 *Surf. Coat. Technol.* **232** 734
- [16] Arab Juneghani M, Farzam M and Zohdirad H 2013 *Trans. Nonferrous Met. Soc. China* **23** 1993
- [17] Eslami M, Golestani-Fard F, Saghaifan H and Robin A 2014 *Mater. Des.* **58** 557

- [18] Chang L M, An M Z, Guo H F and Shi S Y 2006 *Appl. Surf. Sci.* **253** 2132
- [19] Bahadormanesh B and Dolati A 2010 *J. Alloys Compnd.* **504** 514
- [20] Arunsunai Kumar K, Paruthimal Kalaignan G and Muralidharan V S 2013 *Ceram. Int.* **39** 2827
- [21] Sen R, Das S and Das K 2011 *Mater. Charact.* **62** 257
- [22] Zarghami V and Ghorbani M 2014 *J. Alloys Compnd.* **598** 236
- [23] Eslami M, Saghafian H, Golestani-Fard F and Robin A 2014 *Appl. Surf. Sci.* **300** 129
- [24] Ikram Ul Haq *et al* 2013 *Surf. Coat. Technol.* **235** 691
- [25] Bakhit B and Akbari A 2013 *J. Alloys Compnd.* **560** 92
- [26] Wang J-L *et al* 2010 *Trans. Nonferrous Met. Soc. China* **20** 839
- [27] Rostami M *et al* 2013 *Appl. Surf. Sci.* **265** 369
- [28] Zhang H-J *et al* 2013 *Trans. Nonferrous Met. Soc. China* **23** 2011
- [29] Zhou Y-B *et al* 2010 *Trans. Nonferrous Met. Soc. China* **20** 104
- [30] Lei Shi *et al* 2006 *Appl. Surf. Sci.* **252** 3591
- [31] Zhou Y-B and Ding Yuan-Zhu 2007 *Trans. Nonferrous Met. Soc. China* **17** 925
- [32] Lekka M *et al* 2011 *Surf. Coat. Technol.* **205** 3438
- [33] Abdel Aal A, El-Sheikh S M and Ahmed Y M Z 2009 *Mater. Res. Bull.* **44** 151
- [34] Kilic F, Gul H, Aslan S, Alp A and Akbulut H 2013 *Colloids Surf. A* **419** 53
- [35] Ranjith B and Paruthimal Kalaignan G 2010 *Appl. Surf. Sci.* **257** 42
- [36] Wang Junli, Xu Ruidong and Zhang Yuzhi 2012 *J. Rare Earth.* **30** 43
- [37] Golestanifard F, Bahrevar M A and Salahi E 2013 *Materials characterization and analysis methods* (Iran: Central Publication of Iran University of Science and Technology) (in Persian)